Article

Neuron

Neurofilament Light Chain in Blood and CSF as Marker of Disease Progression in Mouse Models and in Neurodegenerative Diseases

Highlights

- Increased NfL in CSF and blood of proteopathic neurodegenerative diseases
- Increased NfL in CSF and blood coincides with onset of proteopathic lesions in brain
- NfL as disease progression and treatment response marker
- Translational value and predictability of current mouse models in clinical settings

Authors

Mehtap Bacioglu, Luis F. Maia, Oliver Preische, ..., Walter Maetzler, Jens Kuhle, Mathias Jucker

Correspondence

jens.kuhle@usb.ch (J.K.), mathias.jucker@uni-tuebingen.de (M.J.)

In Brief

Bacioglu et al. (2016) report NfL increases in CSF and blood of murine models and human α-synucleinopathies, tauopathies, and β-amyloidosis. NfL in bodily fluid constitutes a biomarker of neurodegeneration reflecting the translational value and potential impact of current mouse models in clinical settings.

Bacioglu et al., 2016, Neuron *91*, 1–11
July 6, 2016
http://dx.doi.org/10.1016/j.neuron.2016.05.018

CellPress

Please cite this article in press as: Bacioglu et al., Neurofilament Light Chain in Blood and CSF as Marker of Disease Progression in Mouse Models and in Neurodegenerative Diseases, Neuron (2016), http://dx.doi.org/10.1016/j.neuron.2016.05.018

Neuron
Article

Neurofilament Light Chain in Blood and CSF as Marker of Disease Progression in Mouse Models and in Neurodegenerative Diseases

Mehtap Bacioglu,[1,2,3,10] Luis F. Maia,[1,2,4,10] Oliver Preische,[1,5] Juliane Schelle,[1,2,3] Anja Apel,[1,6] Stephan A. Kaeser,[1,2] Manuel Schweighauser,[1,2,3] Timo Eninger,[1,2,3] Marius Lambert,[1,2] Andrea Pilotto,[1,6] Derya R. Shimshek,[7] Ulf Neumann,[7] Philipp J. Kahle,[1,6] Matthias Staufenbiel,[1,2] Manuela Neumann,[1,8] Walter Maetzler,[1,6] Jens Kuhle,[9,11,*] and Mathias Jucker[1,2,11,*]

[1]German Center for Neurodegenerative Diseases (DZNE), Tuebingen, D-72076 Tuebingen, Germany
[2]Department of Cellular Neurology, Hertie Institute for Clinical Brain Research, University of Tuebingen, D-72076 Tuebingen, Germany
[3]Graduate School of Cellular and Molecular Neuroscience, University of Tuebingen, D-72074 Tuebingen, Germany
[4]Department of Neurology, Hospital de Santo António-CHP, 4099-001 Porto, Portugal
[5]Department of Psychiatry and Psychotherapy, University of Tuebingen, D-72076 Tuebingen, Germany
[6]Department of Neurodegeneration, Hertie Institute for Clinical Brain Research, University of Tuebingen, D-72076 Tuebingen, Germany
[7]Novartis Institutes for BioMedical Research, Novartis Pharma AG, CH-4002 Basel, Switzerland
[8]Department of Neuropathology, University of Tuebingen, D-72076 Tuebingen, Germany
[9]Neurology, Departments of Medicine, Biomedicine, and Clinical Research, University Hospital Basel, CH-4031 Basel, Switzerland
[10]Co-first author
[11]Co-senior author
*Correspondence: jens.kuhle@usb.ch (J.K.), mathias.jucker@uni-tuebingen.de (M.J.)
http://dx.doi.org/10.1016/j.neuron.2016.05.018

SUMMARY

A majority of current disease-modifying therapeutic approaches for age-related neurodegenerative diseases target their characteristic proteopathic lesions (α-synuclein, Tau, Aβ). To monitor such treatments, fluid biomarkers reflecting the underlying disease process are crucial. We found robust increases of neurofilament light chain (NfL) in CSF and blood in murine models of α-synucleinopathies, tauopathy, and β-amyloidosis. Blood and CSF NfL levels were strongly correlated, and NfL increases coincided with the onset and progression of the corresponding proteopathic lesions in brain. Experimental induction of α-synuclein lesions increased CSF and blood NfL levels, while blocking Aβ lesions attenuated the NfL increase. Consistently, we also found NfL increases in CSF and blood of human α-synucleinopathies, tauopathies, and Alzheimer's disease. Our results suggest that CSF and particularly blood NfL can serve as a reliable and easily accessible biomarker to monitor disease progression and treatment response in mouse models and potentially in human proteopathic neurodegenerative diseases.

INTRODUCTION

Proteopathic neurodegenerative diseases are the most common chronic and debilitating disorders of the aging population. They are characterized by pathological hallmarks in brain including region-specific neurodegeneration and deposition of aggregated proteins, namely Tau and amyloid-β (Aβ) in Alzheimer's disease (AD), α-synuclein (αS) in idiopathic Parkinson's disease (IPD), dementia with Lewy bodies (DLB) and multiple system atrophy (MSA), and Tau in progressive supranuclear palsy (PSP) and corticobasal syndrome (CBS). The proteopathic lesions develop at least a decade before the onset of the first symptoms, and this preclinical period is considered the most promising intervention time for disease-modifying therapies (Del Tredici and Braak, 2012; Jack and Holtzman, 2013; Marek et al., 2008; Sperling et al., 2014). To tackle diseases at such early stages, biomarkers that reflect the impact of disease-modifying treatments and that are easily accessible—ideally in blood—are of utmost importance.

Given the difficulty of identifying patients at such preclinical disease stages, well-characterized mouse models hold great translational value. In such genetically induced models, biomarker changes during disease progression or in response to therapy can be directly validated with the brain pathology, thus avoiding the diagnostic uncertainty and interfering comorbidities present in humans. Moreover, the homogeneity of genetically defined mouse models minimizes the interindividual variability and allows the use of mice even in a cross-sectional study design (Barten et al., 2011; Maia et al., 2013, 2015).

A putative biomarker candidate to monitor disease progression and disease-modifying treatments is the neurofilament light chain protein (NfL). Together with the neurofilament medium (NfM) and heavy (NfH) subunits, NfL is one of the scaffolding proteins of the neural cytoskeleton, with important roles in axonal and dendritic branching and growth (Lépinoux-Chambaud and Eyer, 2013; Petzold, 2005). Following CNS axonal damage, NfL levels in the CSF increase and thus are considered as a promising

biomarker of axonal injury in multiple neurological disorders (Kuhle et al., 2015; Neselius et al., 2012; Petzold, 2005). More recently, CSF NfL has also been reported to be elevated in neurodegenerative conditions such as AD, PD, frontotemporal dementia, and amyotrophic lateral sclerosis (Bäckström et al., 2015; Lu et al., 2015; Scherling et al., 2014; Zetterberg et al., 2016).

Here we studied NfL changes in blood, CSF, and brain of a variety of mouse models of proteopathic neurodegenerative diseases. In two murine models of α-synucleinopathy (A53T-αS and A30P-αS tg mice), a model of tauopathy (P301S-Tau tg mice) and a model of cerebral β-amyloidosis (APPPS1 tg mice), we observed robust and early increases of NfL levels in CSF and, remarkably, also blood. Interestingly, in all tg lines high NfL levels in bodily fluids coincided with related pathological changes in the brain. To mechanistically investigate the association between NfL changes in bodily fluids and proteopathic lesions in brain, we experimentally induced or blocked αS and Aβ lesions, respectively. Finally, we show increased NfL levels in CSF and also blood of representative human α-synucleinopathies, tauopathies, and β-amyloidosis. Our findings suggest that CSF and plasma NfL may serve not only as progression marker but also as a biomarker for treatment response in proteopathic neurodegenerative diseases.

RESULTS

Proteopathic Lesions in Transgenic Mouse Brains

To examine onset and progression of brain pathology in A53T-αS, P301S-Tau, and APPPS1 tg mice, brains and spinal cords from different age groups were stained with antibodies against phosphorylated αS, phosphorylated tau, and Aβ, respectively. While 2- to 4-month-old A53T-αS mice did not yet show any αS inclusions, at the age of 6–8 months first lesions became apparent, coinciding with the time of early motor signs (Figure 1A). Thereafter, αS inclusions dramatically increased, and at 8–10 months of age A53T-αS mice became severely impaired and the animals had to be sacrificed. At that time the majority of brainstem including midbrain, pons and medulla, and spinal cord nuclei exhibited αS inclusions (Figure 1A). The remaining brain regions were largely free of αS inclusions.

In P301S-Tau mice, Tau deposits first appeared in the brainstem but did not become prominent until 10–12 months of age. Tau inclusions further increased and mice revealed motor signs at 14–16 months of age when they were analyzed (Figure 1B). At that time Tau inclusions were present in most brainstem and spinal cord nuclei. The remaining brain regions were largely free of Tau inclusions.

In APPPS1 mice, Aβ deposits were already present in the 3 month group, where they were restricted to forebrain regions (mainly neocortex and hippocampus). At 12 and 18 months of age, Aβ deposits were found throughout the entire brain, including brainstem and spinal cord (Figure 1C). No obvious neurological signs were observed in this line up to 18 months of age.

Transgenic Mouse Models Reveal Increased NfL in CSF and Blood

In all three examined mouse models an increase in CSF NfL levels was already observed in asymptomatic stages, and the levels and timing were related to the development of the brain lesions and severity of the neurological signs. Plasma NfL levels were 1/30–1/40 of the CSF levels (Figure 2). The specificity of the assay for murine CSF and plasma NfL was demonstrated by the analysis of NfL-deficient mice (see Experimental Procedures).

In the A53T-αS mice, a significant, more than 10-fold increase in CSF NfL over non-tg controls was already observed in non-symptomatic 2- to 4-month-old mice. Thereafter NfL levels increased dramatically and in 8- to 10-month-old symptomatic mice NfL levels were approximately 1,000-fold higher than in non-tg age-matched controls. Plasma NfL did not yet exhibit a significant increase at 2–4 months of age, but an over 100-fold increase was noted in the A53T-αS mice at the symptomatic stage (Figure 2).

P301S-Tau mice exhibited the first significant increase in CSF NfL levels at 10–12 months of age compared to controls. At 14–16 months of age, when the mice presented the first phenotypical signs, the increase was 20-fold over non-tg control mice. Plasma levels became significantly different at 10–12 months of age also before the mice showed any motor signs (Figure 2).

Consistently, such findings were also observed in APPPS1 mice with significantly higher CSF NfL levels over non-tg controls at both 3 and 12 months of age. Overall, the absolute NfL increase was less than that observed in the A53T-αS and P301S-Tau mice. At 18 months of age the increase in the APPPS1 mice was 10-fold over the age-matched non-tg controls. Plasma NfL appeared also increased at 18 months compared to non-tg controls (Figure 2).

CSF and plasma NfL levels showed a significant positive correlation in all the mouse models whether assessed over all age groups or within same age groups (see Figure S1 available online). Moreover, CSF and plasma NfL correlated strongly with the brain pathology as exemplified in the 6- to 8-month-old A53T-αS mice (Figure S1).

To examine whether NfL levels also change in the brain, brain levels of NfL were measured in aged A53T-αS, P301S-Tau, and APPPS1 mice. However, no significant changes were detected (Figure S2), although histological analyses revealed the expected and previously described NfL-positive neuritic abnormalities in brainstem (for A53T-αS and P301S-Tau mice) and forebrain (APPPS1 mice) consistent with axonal pathology (Figures S3 and S4) (Leroy et al., 2007; Martin et al., 2006; Wirths et al., 2006). Overall, total NfL levels in wild-type (WT) brain were approximately 25,000-fold higher than in CSF and partially elucidate why even a 100- to 1,000-fold increase in CSF NfL is not easily detectable when total brain NfL is analyzed.

Induction of αS Lesions Increases NfL in CSF and Blood of A30P-αS Mice

To confirm NfL changes in CSF and blood of αS tg mice, we used a second αS tg mouse model (A30P-αS) that develops pathology more slowly than the A53T-αS line. Moreover, to explore the mechanistic link of the NfL changes in CSF and blood with the occurrence of the αS inclusions and related neurodegeneration, seeded induction of αS lesions was performed (Figure 3A) (Luk et al., 2012; Mougenot et al., 2012; Schweighauser et al., 2015). To this end, A30P-αS mice either were inoculated with

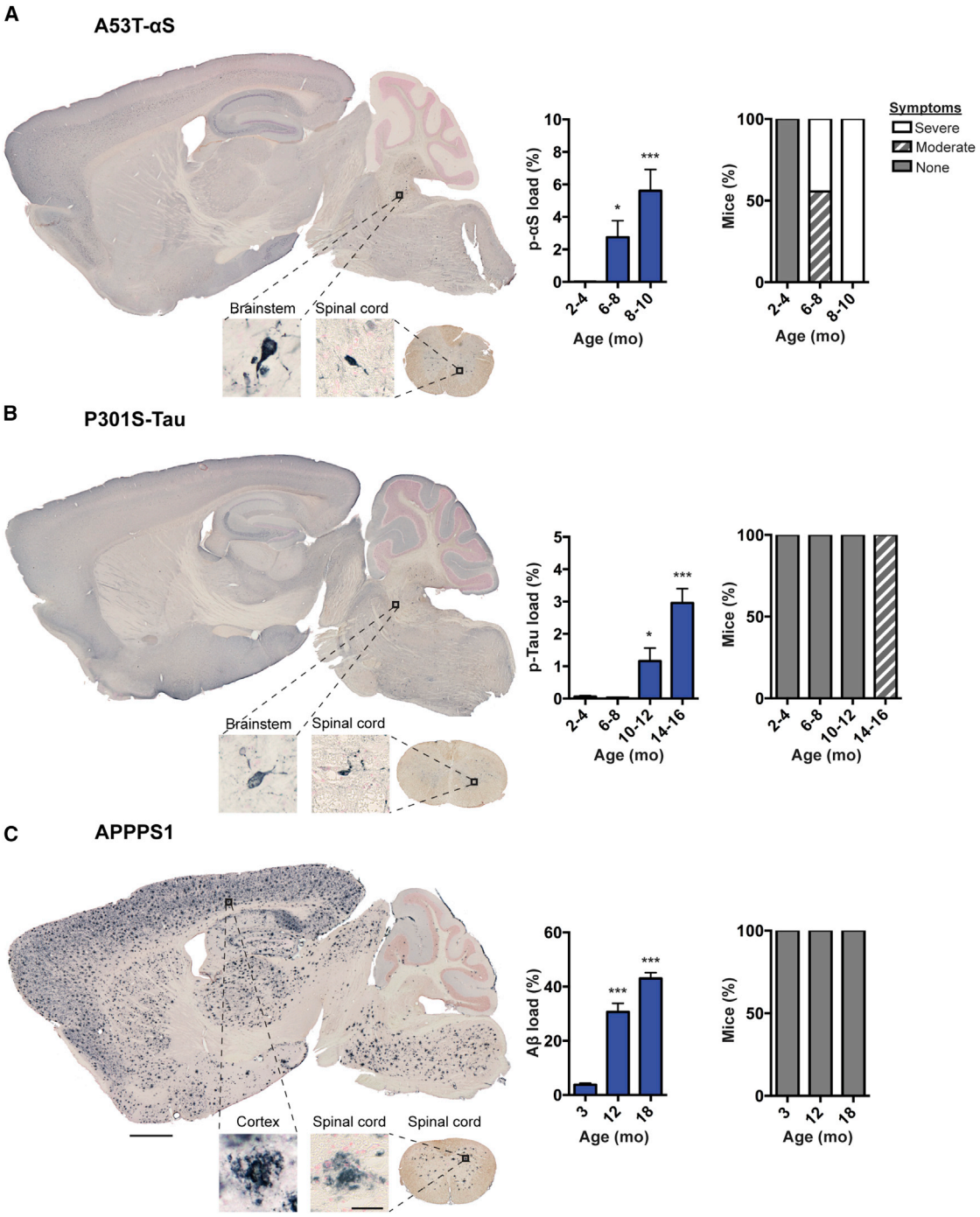

Figure 1. Age-Related Development of Proteopathic Lesions in Brains of α-Synuclein, Tau, and APP tg Mice

(A) Immunostained hyperphosphorylated α-Synuclein (p-αS) aggregates in A53T-αS tg mice (shown is a 9-month-old male mouse).

(B) Immunostained hyperphosphorylated Tau aggregates (p-Tau) in P301S-Tau mice (shown is a 14-month-old male mouse).

(C) Immunostained Aβ deposits in APPPS1 (shown is an 18-month-old male mouse). Nuclear fast red was used as counterstain. Inserts show higher magnifications of αS and Tau inclusions and of extracellular Aβ deposits. Scale bars represent 1,000 μm and 25 μm for insets. The right panels show the quantification of the lesions (p-αS and p-Tau in brainstem, Aβ in cortex) and the occurrence of symptoms in the different age groups. In all mouse models the lesions increased significantly with aging (means ± SEM; n = 5–9 mice per group; for A53T-αS, Kruskal-Wallis, $H[3] = 12.87$, $p = 0.0016$; for P301S-Tau, ANOVA, $F[3,17] = 23.42$, $p < 0.001$; for APPPS1, ANOVA, $F[2,15] = 82.18$, $p < 0.001$). Differences between the youngest and all other age groups were analyzed using Dunn's (for A53T-αS) or Bonferroni's (P301S-Tau and APPPS1) post hoc test for multiple comparisons. *$p < 0.05$, **$p < 0.01$, ***$p < 0.001$). See also Figure S1.

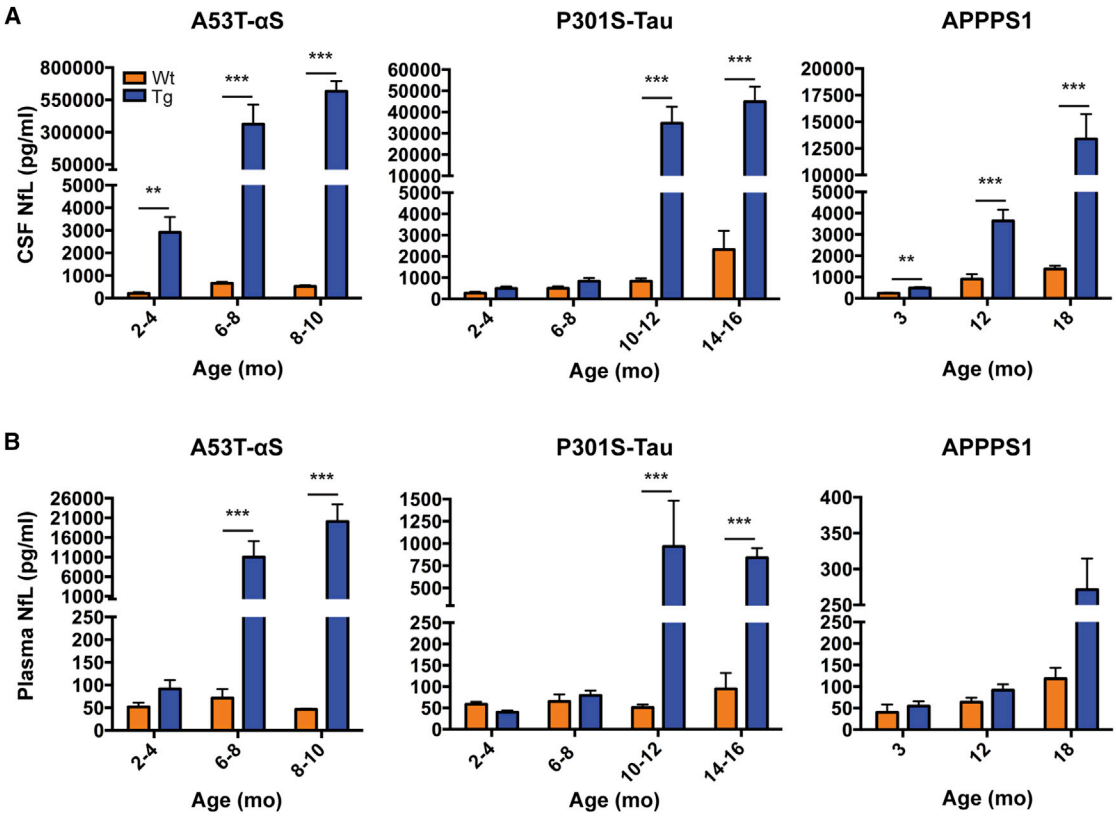

Figure 2. Increase of NfL in CSF and Blood Plasma of α-Synuclein, Tau, and APP tg Mice

(A) CSF NfL and (B) plasma NfL levels in tg mice at different ages in comparison to WT controls. The same tg mice were used as in Figure 1 (n = 5–9 mice per group). For WT mice, n was 4–6 mice/group except for the 14- to 16-month-old WT group, where only 2 mice were available. Means ± SEM are shown. One plasma value was an outlier and excluded from the analysis (see Experimental Procedures). ANOVAs (age × tg) revealed significant age and tg effects and also significant interactions (int) for CSF (A53T-αS, $F_{age}[2,31] = 25.32$, $p < 0.001$; $F_{tg}[1,31] = 160.3$, $p < 0.001$; $F_{int}[2,31] = 10.75$, $p < 0.001$; P301S-Tau, $F_{age}[3,30] = 120.3$, $p < 0.001$; $F_{tg}[1,30] = 181.4$, $p < 0.001$; $F_{int}[3,30] = 35.22$, $p < 0.001$; APPPS1, $F_{age}[2,30] = 151.1$, $p < 0.001$; $F_{tg}[1,30] = 151.0$, $p < 0.001$; $F_{int}[2,30] = 13.48$, $p < 0.001$). Similar results were found for blood plasma (A53T-αS, $F_{age}[2,28] = 12.98$, $p < 0.001$, $F_{tg}[1,28] = 56.20$, $p < 0.001$; $F_{int}[2,28] = 11.86$, $p < 0.001$; P301S-Tau, $F_{age}[3,30] = 19.82$, $p < 0.001$, $F_{tg}[1,30] = 43.12$, $p < 0.001$, $F_{int}[3,30] = 17.82$, $p < 0.001$; APPPS1, $F_{age}[2,30] = 22.35$, $p < 0.001$, $F_{tg}[1,30] = 11.36$, $p < 0.001$, $F_{int}[2,30] = 0.735$, $p > 0.05$). Note that data were log10 normalized for this analysis (see Experimental Procedures). If appropriate, differences between tg and WT for each age group were then compared using Bonferroni's post hoc test for multiple comparisons (**$p < 0.01$, ***$p < 0.001$). Note the much higher NfL levels in CSF and blood of the aged αS mice compared to the Tau mice and in turn to the APPPS1 mice, which corresponds to the observation that the aged αS mice were end-stage symptomatic while the oldest Tau mice were early-stage symptomatic and the APPPS1 mice did not show obvious neurological signs. See also Figures S1–S4.

brain extract derived from aged symptomatic A30P-αS tg mice (Tg extract) or remained noninjected (control). Indeed, Tg-extract-inoculated mice revealed motor signs and had to be analyzed already at 7–8 months of age, while control A30P-αS became symptomatic at 18–22 months of age (Figure 3B). All symptomatic mice, whether analyzed at 18–22 months (control) or 7–8 months (Tg-extract induced) revealed severe and equivalent αS pathology in the brainstem (Figure 3C). As a further control, A30P-αS mice inoculated with aged WT extract did not show any anticipation of the clinical or the pathological phenotype when analyzed at 10 months of age.

Measurements of NfL in both CSF and plasma from noninjected A30P-αS mice revealed a very robust age-related increase (Figure 3D) in magnitude similar to that the A53T-αS mice (Figure 2) but only reached at 18–22 months of age. Injection of the A30P-αS mice with tg-extract shifted this increase to 7–8 months, in support of a mechanistic link between the αS lesions and fluid NfL levels (Figure 3D).

Inhibition of Aβ Lesions Decreases NfL in CSF and Blood of APPPS1 Mice

While inducing proteopathic lesions increased NfL levels in bodily fluids, reducing such lesions would be expected to reduce NfL levels. To investigate this, we took advantage of APPPS1 mice that have been treated with a potent BACE1-inhibitor to inhibit Aβ production and thus the buildup of Aβ deposits and associated pathologies (Figures 4A and 4B) (Neumann et al., 2015). Indeed, BACE1-inhibitor treatment of APPPS1 mice for 6 months revealed a 71% reduction of Aβ deposition in brain compared to control mice (Figure 4B). When brain Aβ was measured by immunoassay, a 97% and 94% reduction of Aβ40 and Aβ42 was found (results not shown). Consistently, BACE1-inhibitor-treated mice

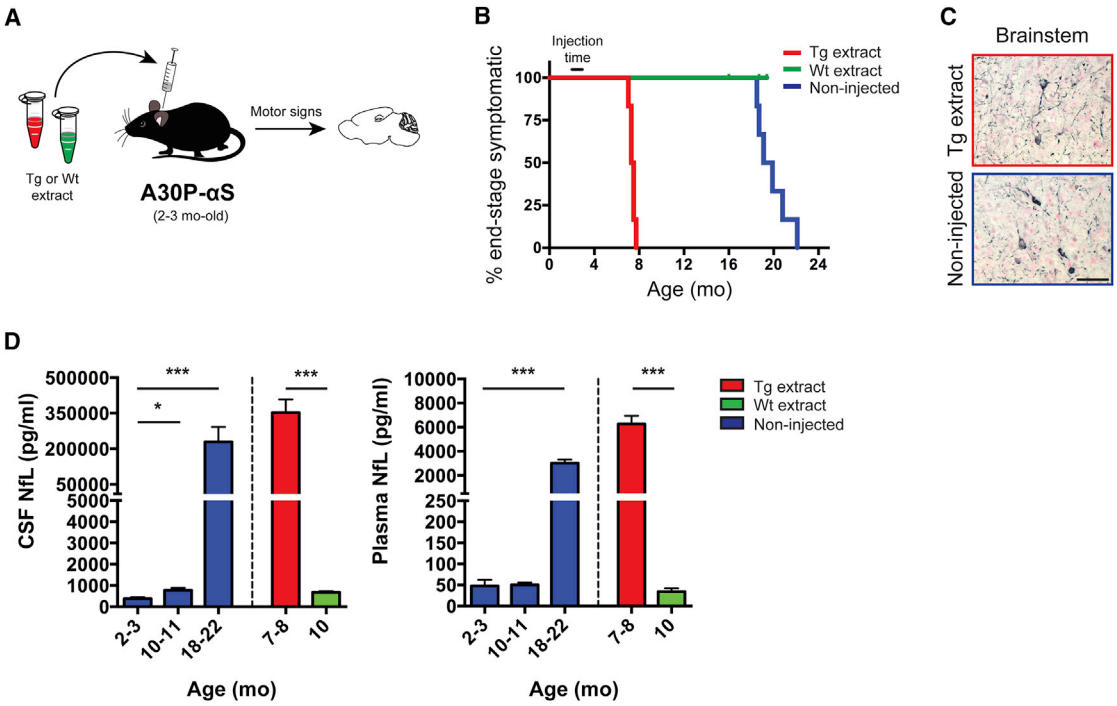

Figure 3. Inducing α-Synuclein Lesions in A30P-αS Transgenic Mice Increases NfL in CSF and Blood

(A) Schematic illustration of brainstem injection of brain extract derived from aged symptomatic A30P-αS tg mice (tg extract) or aged non-tg WT mice (WT extract) in young 2- to 3-month-old A30P-αS tg mice. Tg-extract-injected A30P-αS tg mice were analyzed after displaying motor signs. WT-extract-injected mice did not yet display motor signs at the time of writing this manuscript. Nevertheless, as a control, 3 WT-extract-injected mice were analyzed at 10 months of age (7 months after inoculation).

(B) Survival curve of A30P-αS mice injected with tg extract (red curve; median survival 7.4 months, n = 6) and WT extract (green curve; all but the 3 mice mentioned above are still alive); for comparative reasons, noninjected A30P-αS tg mice were added (blue curve; median survival 19.5 months, n = 6) ($p < 0.017$, log rank test with Bonferroni correction).

(C) Immunostaining for αS (pSer129) in brainstem of symptomatic tg-extract-injected A30P-αS mice (shown is a 7-month-old female mouse) and symptomatic noninjected controls (shown is a 19-month-old male mouse) reveals similar perinuclear inclusions and dystrophic neurites. No αS pathology was observed in brainstem of the 10-month-old WT extract-injected mice (data not shown). Scale bar, 50 μm.

(D) CSF and blood plasma NfL levels in A30P-αS mice (blue bars; n = 5–6/group; ANOVA, $F(2,14) = 287.4$ for CSF and $F(2,13) = 212.6$ for plasma, respectively, ps < 0.001). Bonferroni's post hoc comparison revealed significant increase in CSF and plasma levels in the 10- to 11- and 18- to 22-month-old groups (*$p < 0.05$, ***$p < 0.001$). Symptomatic tg-extract-injected A30P-αS mice (n = 6), despite being only 7–8 months old (red bar) revealed significantly higher NfL levels both in CSF and blood compared to the WT-extract-injected A30P-αS mice (n = 3) (which were analyzed at 10 months of age, see above) (t test, ***$p < 0.001$). In total, one CSF and two plasma values were outliers and excluded from the analysis (see Experimental Procedures). All data represented as group means ± SEM.

had 63% lower CSF NfL levels when compared to the control APPPS1 mice (Figure 4C). Plasma NfL levels of BACE1-inhibitor-treated mice were also lowered, albeit the 20% difference did not reach statistical significance (Figure 4D).

Increased NfL in CSF and Blood of Human α-Synucleinopathies, Tauopathies, and β-Amyloidosis

To study whether NfL is also increased in CSF and blood in human diseases with αS, Tau, and Aβ lesions, cohorts of normal healthy controls were compared with cohorts of typical α-synucleinopathies (IPD, DLB, MSA), tauopathies (PSP, CBS) and β-amyloidosis/tauopathy (mild cognitive impairment [MCI], AD) (Table S1). Albeit smaller than in the mouse models, increases in CSF NfL were found in all disease cohorts compared to the healthy controls with the exception of IPD (Figure 5A). For blood analysis, serum rather than plasma was available from the human subjects. However, previous results have found similar NfL levels and a high correlation of NfL levels between human serum and plasma (see Experimental Procedures). Strikingly, and again similar to mice, NfL in blood was increased in all disease groups but IPD (Figure 5B).

The increase of NfL in both CSF and blood in patients was 1.5- to 5.5-fold as compared with healthy controls and therefore much smaller than in mice. Notably, however, and similar to the mouse models, there was a significant correlation between human CSF and blood NfL levels in the controls (Figure S5), and the correlation also reached significance in many of the disease groups (Table S1). The ratios of blood/CSF NfL levels in the human samples were 1/30–1/70 (Figure 5) and were in the same range as in the mouse models (1/30–1/40; see above and Figure 2). Notably, however, NfL levels in both CSF and blood of healthy human controls were approximately 2.5 times lower than in the aged non-tg control mice.

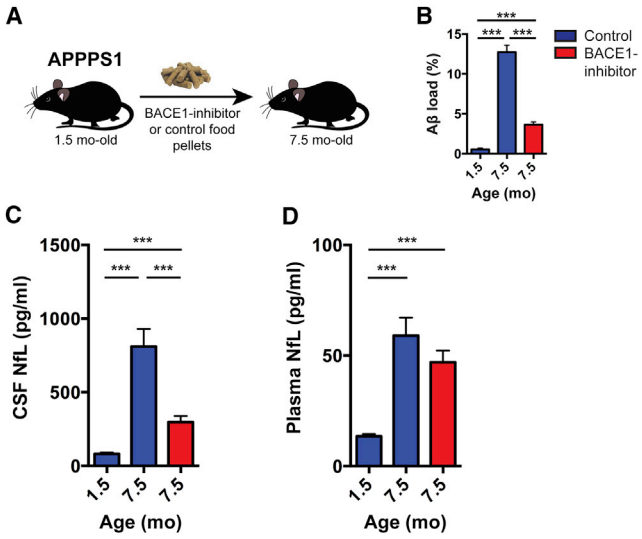

Figure 4. Reducing Aβ Deposition in APPPS1 Mice Prevents the NfL Increase in CSF

(A) Schematic illustration for BACE1-inhibitor treatment of APPPS1 mice. Mice were treated with BACE1-inhibitor or control food pellets for 6 months.

(B) Stereological quantification of cortical immunoreactive (dark blue) Aβ staining (Aβ load) in these mice revealed a significant reduction in Aβ plaque deposition in 7.5-month-old BACE1-inhibitor treated mice compared to age-matched controls (n = 8–10/group; ANOVA, $F[2,24] = 154.9$, $p < 0.001$). Differences between the groups were analyzed using Bonferroni's post hoc test for multiple comparisons, ***$p < 0.001$).

(C) Measurement of NfL in the CSF of the same mice as in (B) revealed reduced NfL levels in the BACE1-inhibitor treated mice compared to 7.5-month-old control mice (ANOVA, $F[2,24] = 57.51$, $p < 0.001$; Bonferroni post hoc comparison ***$p < 0.001$).

(D) In blood NfL levels significantly increased between 1.5 and 7.5 months of age and were somewhat reduced in the 7.5-month-old BACE1-inhibitor treated mice compared to 7.5-month-old control mice, but the reduction was not significant (ANOVA, $F[(2,23] = 58.17$, $p < 0.001$, Bonferroni's post hoc comparisons, ***$p < 0.001$). All data presented are group means ± SEM.

Finally, correlation analyses were done between CSF NfL and CSF Aβ42 (the 42 amino acid long Aβ species) and Tau, which were available for the majority of the human samples (Table S1). No significant correlations were found between CSF Aβ42 and CSF NfL in any of the groups. A positive correlation for CSF Tau and CSF NfL was found in the healthy controls ($r_s = 0.39$, $p < 0.05$), IPD ($r_s = 0.37$, $p < 0.05$), MSA ($r_s = 0.60$, $p < 0.05$), but surprisingly not in AD. There was also a significant correlation between cognitive performance on Mini-Mental State Examination (MMSE) and CSF NfL ($r_s = -0.45$, $p < 0.05$) or blood NfL ($r_s = -0.45$, $p < 0.05$) in AD, indicating that AD severity may be reflected in increased NfL levels.

DISCUSSION

We found that NfL levels are elevated in both CSF and blood of mouse models that replicate the most frequent neurodegenerative proteopathic lesions (αS, Tau, and Aβ). In all models, NfL increased, coinciding with the emergence and progression of the corresponding brain lesions. In two of the models (A30P-αS and APPPS1), we explored the link between NfL changes and lesion development by experimentally inducing αS and blocking Aβ lesions. Consistently, NfL levels increased in response to induction of αS pathology and declined as Aβ pathology was reduced. These findings suggest that CSF and plasma NfL may serve not only as disease progression markers but also as treatment response biomarkers for proteopathic lesion-induced neurodegeneration. From a translational perspective, our preclinical results are supported by elevated NfL in CSF and notably also in blood of patients with α-synucleinopathies, tauopathies, and β-amyloidosis. Thus, the present finding that an easily accessible blood biomarker can track CNS neurodegeneration is a major advantage for preclinical mouse model research and implies that NfL changes in bodily fluids may serve as a progression and treatment response marker for human neurodegenerative diseases.

For the present study, we first set out to adapt and validate a previously published NfL assay (Gaiottino et al., 2013) for murine samples and small volumes. This assay was chosen for further development because it also recognizes human NfL and thus is of added translational value. Using this assay we found a strong correlation between CSF and plasma NfL in the mouse models, suggesting that most of the NfL in blood derives from the CNS. The fact that the rise in CSF NfL levels occurs earlier and with greater magnitude compared to the NfL changes in blood is also supportive of this interpretation.

Remarkably, NfL increases became significant in mouse CSF and to some extent also in blood before obvious neurological signs developed. Although future studies with more age groups per mouse line will refine the development over time, it is likely that the increases of NfL in CSF and blood tightly coincide with the occurrence of the proteopathic lesions in brain. Consistently, NfL levels correlated positively with the protein deposits in each of the models, and experimental increase or decrease of the deposits shifted NfL accordingly. An exception was found for the 2- to 4-month-old A53T-αS mice that have not yet revealed histologically detectable αS inclusion but exhibited increased NfL levels. This observation could be explained by the occurrence of pathogenic αS aggregates that escape histological detection.

Since increased CSF and plasma NfL levels were found in all the models analyzed, it obviously is not specific for aggregates of αS, Tau, or Aβ, suggesting secondary insults as common denominator. Increased NfL in bodily fluids is thought to reflect axonal injury, axonal pathology, or axonal dysfunction (Petzold, 2005), and indeed axonal pathology has been described in αS-, Tau-, and APP-tg mouse models (e.g., Lewis et al., 2000; Phinney et al., 2003; Spittaels et al., 1999; van der Putten et al., 2000; Wirths et al., 2006) and was also found in the aged mice of the present study. The more prominent NfL increase in both CSF and blood in the αS- and Tau-tg lines compared to the APPPS1 model may reflect the more rapid disease progression and the predominant brainstem and spinal cord pathology of these αS and Tau lines. Brainstem and in particular spinal cord harbor thick-caliber myelinated motor neuron axons that are rich in NfL (Liu et al., 2004; Petzold, 2005; Yuan et al., 2012a). Consistently, in ALS patients CSF NfL levels are at least 3-fold higher compared to AD patients (Gaiottino et al., 2013; Steinacker et al., 2016; Zetterberg et al., 2016). Moreover, patients with multiple sclerosis

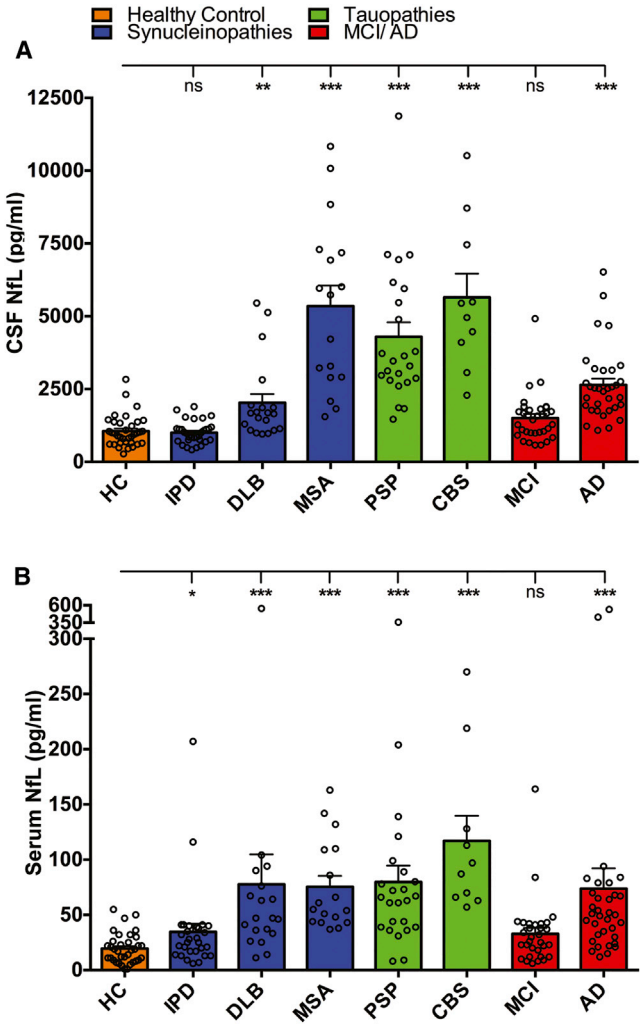

Figure 5. Increase of NfL in CSF and Blood Serum of Human α-Synucleinopathies, Tauopathies, and β-Amyloidoses

(A) NfL in CSF and (B) NfL in serum of healthy controls (HC, n = 35), idiopathic Parkinson's disease (IPD, n = 32), dementia with Lewy bodies (DLB, n = 20), multiple system atrophy (MSA, n = 17), progressive supranuclear palsy (PSP, n = 24), corticobasal syndrome (CBS, n = 10), mild cognitive impairment (MCI, n = 33), and Alzheimer's disease (AD, n = 34) (see Table S1 for subject details). Group means ± SEM and individual values are presented. ANCOVA, controlling for age, revealed for CSF NfL: $F(7,193) = 44.1$, and serum NfL: $F(7,189) = 19.5$, both $p < 0.001$; Bonferroni's post hoc comparison was performed between HC and all the disease groups for CSF and serum. Note: data were log10 transformed for this analysis. Outliers were excluded (CSF n = 2; serum n = 4) (see Experimental Procedures). In addition, one CSF sample was not available, and three serum samples did not yield any signal/were below level of detection. (*$p < 0.05$, **$p < 0.01$, ***$p < 0.001$; ns, not significant). See also Figure S5.

experiencing an acute spinal cord-located relapse have significantly higher CSF NfL than patients with brain-localized relapses (Kuhle et al., 2013). Thus, the present observations are consistent with NfL release into the CSF and blood from dysfunctional or degenerating axons, although the exact mechanism remains unclear.

To extend our observations from the mouse models to human diseases, we used the same immunoassay to measure NfL in human patients with (proteopathic) neurodegenerative disorders. Consistent with our findings in mice and in line with previous observations, we found an increase in CSF NfL in α-synucleinopathies (MSA and DLB), tauopathies (PSP and CBS), and mixed β-amyloidosis/tauopathy (AD and MCI). In IPD, CSF NfL was not increased, which may reflect not only the slower progression of neurodegeneration in IPD but also the more topographically confined neurodegeneration compared to the atypical parkinsonian syndromes (APS), including DLB, MSA, PSP, and CBS (Prodoehl et al., 2013). The difference between IPD and APS in CSF NfL (baseline area under the receiver operating characteristic curve [AUC] = 0.93, specificity 87%, sensitivity 88%) further supports the impending role of CSF NfL to discriminate IPD from APS (e.g., Sako et al., 2015). Moreover, the observation that increased CSF NfL levels are also reflected in blood suggests that even blood NfL levels may discriminate IPD from APS (AUC 0.81, specificity 76%, sensitivity 81%).

Remarkably, our results reveal that NfL levels in AD are elevated not only in CSF but also in blood. Although the increase did not reach significance in the MCI group (which could be due to the clinical heterogeneity of MCI subjects), it is likely that not only CSF NfL (Zetterberg et al., 2016) but also blood NfL may serve as a biomarker for AD progression, as has recently been suggested for PSP (Rojas et al., 2016). The reduced CSF and blood NfL levels after BACE1-inhibitor treatment of APPPS1 mice suggest that NfL may become an easily accessible biomarker to monitor treatment response in current and future clinical trials in AD (Vassar, 2014).

While in the mouse models most of the blood NfL likely derives from brain (see above), the origin of NfL in human blood is less clear. The NfL plasma/CSF ratio in humans (1/30–1/70) is in a similar range as in mice (1/30–1/40), and also in humans a correlation between CSF and blood NfL was found, which favors the argument that most of the blood NfL in humans is also derived from the brain. However, it is possible that comorbidities of age-related neurodegenerative diseases influence NfL levels in blood.

More recently, in addition to being part of the axonal cytoskeleton protein complex, NfL has been suggested as an integral component of synapses (Yuan et al., 2015), and synapse loss may thus contribute to the increased NfL levels in CSF and blood. Nevertheless, NfL is also present in CSF and blood of wild-type mice and healthy humans. Such findings may reflect not only the putative axonal remodeling but also ongoing synapse remodeling and thus are the basis for the NfL steady-state level in bodily fluid. Additionally, the present study revealed an age-related increase in NfL in the CSF and blood of the wild-type mice, and such an increase has also been observed in (healthy) humans (Vågberg et al., 2015). The observation that CSF and blood NfL levels are 2- to 3-fold higher in aged non-transgenic mice compared to aged human controls may indicate that ongoing turnover of axons and synapse remodeling is higher in mice compared to humans and/or that there are differences in NfL degradation in bodily fluids between the two species.

Although the present study focused on NfL, other neurofilament subunits may have the potential to complement and refine

NfL as a bodily fluid marker of proteopathic neurodegenerative diseases. Indeed, phosphorylated NfH (pNfH) in CSF and blood has been reported to track disease progression in ALS and other diseases (Boylan et al., 2013; Petzold, 2005). Phosphorylated NfH has also been reported to increase in blood of mouse models with superoxide dismutase 1 inclusions, although assay sensitivity did not allow measurement of NfH in non-tg control mice, or samples required preanalytical treatment to overcome matrix effects (Boylan et al., 2009; Lu et al., 2012).

In summary, the common increase of NfL in CSF and blood among mouse models of proteopathic lesions and in human neurodegenerative diseases argues that NfL may become a key biomarker for disease progression. The fact that NfL levels in CSF and even blood are sensitive to experimental manipulations or targeted therapies of the proteopathic lesions makes NfL a primary biomarker to monitor treatment response in preclinical research with potential clinical impact.

EXPERIMENTAL PROCEDURES

Mice

A53T-αS (Thy1-hA53T-αS) (van der Putten et al., 2000), A30P-αS (Thy1-hA30P-αS) (Neumann et al., 2002), P301S-Tau (Thy1-P301S-Tau) (Allen et al., 2002), and APPPS1 (Thy1-hKM670/671NL-APP; Thy1-hL166P-PS1) (Radde et al., 2006) transgenic (tg) and age-matched non-tg WT mice were used. All mice were bred at the Hertie Institute for Clinical Brain Research. For A53T-αS, A30P-αS, and P301S-Tau mice, female and male mice were used, with balanced gender within the groups. For APPPS1, only male mice were used. All mice were maintained on a C57BL/6 background and kept under specific pathogen-free conditions. NfL-deficient mice (*NFL*$^{-/-}$), generously provided by R. Nixon (NKI, Orangeburg, NJ) (Yuan et al., 2012b), were used to assess the specificity of the NfL immunoassay for murine samples (CSF, blood plasma, and brain tissue). The experimental procedures were carried out in accordance with the veterinary office regulations of Baden-Wuerttemberg (Germany) and approved by the local Animal Care and Use Committees.

Assessment of Neurological Phenotype in Mice

A53T-αS, A30P-αS, and P301S-Tau develop neurological/motor signs around 6, 16, and 14 months of age, respectively (Allen et al., 2002; Neumann et al., 2002; van der Putten et al., 2000). The phenotype includes tremor, unsteady gait, hind-limb paresis and clasping, and general muscle weakness. Depending on severity of the phenotype, mice were staged into early-stage symptomatic (detectable tremor and unsteady gait; symptomatic score 0.5) and end-stage symptomatic (severe tremor and unsteady gait, hind-limb clasping and paresis; at this time all animals were sacrificed; symptomatic score 1.0). For A53T-αS mice, both early-stage symptomatic and end-stage symptomatic were included in the study. For P301S-Tau mice, only early-stage symptomatic mice were available. APPPS1 mice (Radde et al., 2006) do not show obvious neurological signs/phenotype in the home cage up to 18 months of age, when the mice were sacrificed. Loss of body weight compared to the non-tg controls was also assessed as a general marker for the wellbeing of the tg mice.

Seeded Induction of α-Synuclein Lesions in Mice

Brains of symptomatic end-stage female A30P-αS mice (16–20 months old, n = 5) were dissected, and the brainstem was immediately fresh-frozen on dry ice. Tissue was pooled from the mice, homogenized (Precellys 24, Bertin Technologies, France) at 10% (w/v) in sterile PBS (Lonza, Switzerland), vortexed, and centrifuged at 3,000 × g for 5 min. The supernatant was aliquoted and immediately frozen. Wild-type seeding extract was derived from an aged (24–26 months old) non-tg male B6 mouse and prepared from the entire brain without cerebellum (Meyer-Luehmann et al., 2006; Schweighauser et al., 2015).

Intracerebral injections of the extract were done into young 2-3 month-old A30P-αS male or female mice. Host mice were anesthetized with a mixture of ketamine/xylazine (ketamine 100 mg/kg, xylazine 10 mg/kg) in saline and carprofen (5 mg/kg body weight) was administered prior to surgery. Unilateral stereotactic injections of 1 μl brain extract were made with a Hamilton syringe into the brainstem (AP −4.0 mm, L ± 1.0 mm, DV −3.5 mm). Injection speed was 1 μl/min, and the needle was kept in place for an additional 2 min before it was slowly withdrawn. The surgical area was cleaned with sterile PBS, and the incision was sutured. The mice were kept under infrared light and monitored until they had recovered from anesthesia. After recovery from surgery, mice were monitored regularly and sacrificed either upon the onset of symptoms (see above) or at predetermined time points after surgery.

BACE inhibitor treatment in mice

Male APPPS1 mice (1.5 months of age) were fed ad libitum with food pellets containing a BACE1-inhibitor (NB-360; 0.5 g/kg food pellets; Neumann et al., 2015) or control pellets without the inhibitor for a treatment period of 6 months. Mice were sacrificed at 7.5 months of age.

CSF and Blood Collection in Mice

CSF collection was done as described previously, adopting the standards set by the Alzheimer's Association external quality control program for human CSF biomarkers (Maia et al., 2015; Mattsson et al., 2011) with modifications. Briefly, after anesthetizing the mice with a mixture of ketamine/xylazine (ketamine 100 mg/kg, xylazine 10 mg/kg), CSF was immediately collected from the cisterna magna. Typically 15–20 μl CSF were collected. CSF samples were then centrifuged at 13,000 × g for 30 s (2,000 × g for 10 min for the BACE1-Inhibitor study and the αS seeding study), assessed macroscopically for blood contamination, aliquoted (5 μl), and stored at −80°C until use. Blood-contaminated samples were not analyzed. After CSF collection, blood was obtained by heart puncture with heparinized syringes and centrifuged at 2,000 × g for 10 min to obtain plasma. Plasma samples were then aliquoted (70 μl) and stored at −80°C until use.

Brain and Spinal Cord Collection from Mice

Anesthetized mice and corresponding controls were perfused with ice-cold sterile PBS except for the APPPS1 mice in Figure 1 which were not perfused. Brains were removed, and one hemibrain was snap-frozen on dry ice and stored at −80°C until use. The other hemibrain was fixed in 4% paraformaldehyde (PFA) in PBS for 48 hr at 4°C, immersed in PBS with 30% sucrose for an additional 48 hr at 4°C, snap-frozen in 2-methylbutane, and stored at −80°C. In a subset of mice, spinal cord was collected as follows: anesthetized mice were initially perfused with ice-cold sterile PBS followed by a 4% PFA perfusion. Then brains and spinal cords were dissected and immersed fixed for 4 hr in 4% PFA. Spinal cords were separated into cervical, thoracic, and lumbar regions. Brains and separated spinal cord regions were embedded in paraffin. Paraffin-embedded brains and spinal cords were stored at room temperature until use.

Histology and Immunohistochemistry of Mouse Brain and Spinal Cord

Brains were cut into 25 μm-thick sections using a freezing-sliding microtome (Leica SM 2000R). The sections were collected in cryoprotectant (35% ethylene glycol, 25% glycerol in PBS) for storage at −20°C. Paraffin-embedded tissue was serially cut into 10 μm-thick sections using a microtome (Thermo Scientific, Microm HM 325), directly transferred on SuperFrost Plus glass slides, incubated overnight at 60°C and deparaffinized before histological analysis. Antigenity was enhanced by boiling the sections in 10 mM citrate buffer (1.8 mM citric acid, 8.2 mM trisodium citrate [pH 6.0]) at 90°C for 35 min for all the antibodies listed below. Immunohistochemistry was performed according to standard protocols with the Vectastain Elite ABC Kit (Vector Laboratories, Burlingame, CA, USA). The following antibodies were used: rabbit monoclonal pS129 antibody (1:750; EP1536Y, Abcam) specific to α-synuclein phosphorylated at ser-129, mouse monoclonal AT8 antibody (1:1,000; Thermo Scientific) specific to Tau phosphorylated at ser-202 and thr-205, rabbit polyclonal NT12 or CN5 antibody (both 1:2,000; Eisele et al.,

2010) to Aβ, and mouse monoclonal antibody against NfL (1:1,000, Chemicon). Sections were counterstained with nuclear fast red according to standard protocols. For Bielschowsky silver stain, paraffin-embedded sagittal brain and transversal spinal cord sections were used.

Stereological Quantification of αS, Tau, and Aβ Lesions on Murine Brain Sections

The areal density of phospho-αS (pS129), phospho-Tau (AT8), and Aβ immunoreactive lesions was quantified in random-systematic set of every 12th section through the specific brain regions: brainstem for Tau and αS, and neocortex for Aβ. Stereological analysis was performed using a Zeiss Axioskop 2 microscope equipped with a motorized *x-y-z* stage coupled to a videomicroscopy system and the Stereo Investigator software (MicroBrightField Inc.). Researchers who were blinded to the age groups performed the analysis. The areal fractions were determined at several focal planes and calculated from the 25 μm-thick sections.

Human Subjects

A total of 205 CSF/serum pairs from the Neuro-Biobank Tuebingen were included (www.hih-tuebingen.de/ueber-uns/core-facilities/biobank/researchers/). Thirty-five were from healthy controls (HC) and 170 from patients with the different proteopathic neurodegenerative diseases as follows: IPD (n = 32), DLB (n = 20), MSA (n = 17), PSP (n = 24), CBS (n = 10), MCI (n = 33), and AD (n = 34) (see Table S1 for demographic and clinical data). HC donated biomaterial to the biobank in the course of other clinical studies (n = 20), or as patients with headache or lumbar back pain to exclude vascular (n = 9) or inflammatory processes (n = 6), respectively. MCI was diagnosed according to published criteria (Winblad et al., 2004). AD was diagnosed according to the NIA-AA-criteria (McKhann et al., 2011). IPD and APSs were classified according to the currently used criteria for the respective form of parkinsonism (Eggert et al., 2012). Information regarding age, disease onset, and disease duration was extracted from the database. Mini Mental State Examination (MMSE), Hoehn and Yahr scale (H&Y), motor part of the Unified Parkinsons Disease Rating Scale (UPDRS-III), and Montreal Cognitive Assessment (MoCA) scores were done on the same day of biomaterial collection. The study was approved by the ethics committee of the Medical Faculty, University of Tuebingen (Tuebingen, Germany). All participants, or their next of kin in the case of relevant cognitive impairment (MMSE score <18), provided a written informed consent.

CSF and Blood Collection in Human Subjects

CSF and serum collection was performed according to standardized protocols (Maetzler et al., 2011). In brief, lumbar puncture and blood collection was performed between 08.00 and 10.00 AM after overnight fasting. Serum (2,000 × g) and CSF (4,000 × g) were centrifuged for 10 min at 4°C and stored at −80°C within 60 min after collection. Only samples with normal routine CSF diagnostics were included in the study (leukocytes <4 × 10^6/L; IgG index CSF /serum <0.6); slightly increased CSF albumin levels (up to 450 μg/mL) were accepted and used.

Electrochemiluminescence Immunoassay to Measure NfL in Mice and Humans

NfL concentrations in brain tissue, CSF, and blood (plasma and serum) were measured in duplicates using a previously described and validated electrochemiluminescence (ECL) immunoassay (capture monoclonal antibody: 47:3; biotinylated detector monoclonal antibody: 2:1, UmanDiagnostics AB, Umeå, Sweden; Gaiottino et al., 2013) with some modifications.

Murine CSF (5 μl) was prediluted 1:14 in sample diluent (tris buffered saline (TBS) containing 1% BSA, 0.1% Tween 20 [pH 7.5]) before analysis. Murine plasma samples were prediluted 1:2 in sample diluent. To measure NfL in brain, fresh-frozen hemibrains were homogenized (Precellys-24, Bertin Technologies, France) at 10% (w/v) in homogenization buffer (50 mM Tris [pH 8.0], 150 mM NaCl, 5 mM EDTA, and Pierce protease and phosphotase inhibitor cocktail from Thermo Scientific). The homogenized brain tissue was centrifuged at 25,000 × g, 4°C, for 1 hr. The supernatant was aliquoted and diluted 1:1,000 in sample diluent. Parallelism and linearity of the assay (at the given dilutions) for murine CSF, plasma, and brain samples were confirmed by serial dilution experiments (Valentin et al., 2011). The specificity of the assay for murine NfL was tested using different samples (CSF, blood, brain tissue) from NfL-deficient mice (see above). In all samples from NfL-deficient mice ($NfL^{-/-}$; n = 3), NfL was undetectable (assay signals in two repeat experiments equal or lower than signal of blank), whereas WT littermate mice (n = 2) had detectable levels (CSF, 210 and 322 pg/ml; plasma, 31.8 and 31.5 pg/ml), which were in the range of all the other non-tg mice of the same age assessed in the present study.

Human CSF and serum measurements were slightly modified by using a ready-to-use ELISA reagent (Mabtech AB, Nacka Strand, Sweden) as sample diluent. Unfortunately, plasma was not available from the human subjects. However, NfL levels from matched human serum and plasma of healthy controls show a high correlation (n = 25, Spearman r = 0.93, p < 0.0001) and strong agreement using Bland-Altman method comparison (bias, 3.92; serum-plasma; 95% confidence interval [CI], −2.41, 10.25; 95% limits of agreement, −26.15, 33.99; J.K., unpublished data; see also Lu et al., 2015).

For both mice and humans, CSF and blood samples from the same individuals were assessed on the same plate. Samples from different mouse strains, ages, and human diseases were evenly distributed across different plates. Samples with coefficients of variation (CVs) above 20% between the measured concentrations in the duplicate determinations were reanalyzed. In the case of few murine samples with limited volumes and with NfL values above the highest calibrator (10,000 pg/ml), concentrations were extrapolated from the standard curve. Intermediate precision (between-run precision) and repeatability (within-run precision) for the murine sample measurements ranged between 7.5%–14.9% and 5.5%–8.9% and for the human sample measurements between 8.4%–14.7% and 6.3%–9.1%, respectively, for three human serum control samples measured in duplicate on every 96-well plate. All NfL measurements were done blinded for age and genotype of the mice and for diagnosis and clinical data from the human subjects.

Statistical Analysis

The distribution of data was assessed either with Kolmogorov-Smirnov test for mouse samples or with D'Agostino & Pearson omnibus normality test for human samples. Outliers were detected with ROUT test (Q = 1) and excluded from the analysis and are indicated in the figure legends. Non-normally distributed data were analyzed with nonparametric tests (Kruskal-Wallis). For CSF and blood NfL values, base10 logarithmic transformation was computed to normalize the data and then analyzed with parametric statistical tests (ANOVA or ANCOVA with Bonferroni's post hoc test). In all cases, statistical significance was set at p < 0.05. GraphPad Prism version 6 (GraphPad Software, La Jolla, California USA) and JMP software (Version 11.2.0; SAS Institute Inc., Cary, North Carolina, USA) were used for statistical analysis of mouse and human data, respectively. All graphics were generated with GraphPad Prism version 6 and presented with mean and SEM.

SUPPLEMENTAL INFORMATION

Supplemental Information includes five figures and one table and can be found with this article at http://dx.doi.org/10.1016/j.neuron.2016.05.018.

AUTHOR CONTRIBUTIONS

M.B., L.F.M., O.P., J.S., S.A.K., M.S., T.E., M.L., M.N., A.P., and J.K. performed the experimental work. M.B., L.F.M., A.A., and M.J. carried out the statistical analysis. D.S., U.N., P.J.K., M.S., W.M. provided crucial research reagents. M.B., L.F.M., J.K., and M.J. designed the study and with the help of all other authors prepared the manuscript.

ACKNOWLEDGMENTS

We would like to thank M. Goedert (MRC, Cambridge, UK) and D. Yuan and R. Nixon (NKI, Orangeburg, NJ) for generously providing P301S-Tau tg mice and NfL null mice, respectively; Peter Martus and Christoph Laske for advice and comments to the manuscript; and Ulrike Obermueller, Yvonne Eisele (now San

Diego), Claudia Schaefer, Manuel Goedan, Christian Barro, and Marguerite Limberg for experimental help. This work was supported by the MetLife Foundation, New York (M.J.), ECTRIMS Research Fellowship Program, University of Basel (J.K.), Swiss MS Society (J.K.), and Swiss National Research Foundation (J.K.).

Received: January 15, 2016
Revised: April 4, 2016
Accepted: May 10, 2016
Published: June 9, 2016

REFERENCES

Allen, B., Ingram, E., Takao, M., Smith, M.J., Jakes, R., Virdee, K., Yoshida, H., Holzer, M., Craxton, M., Emson, P.C., et al. (2002). Abundant tau filaments and nonapoptotic neurodegeneration in transgenic mice expressing human P301S tau protein. J. Neurosci. *22*, 9340–9351.

Bäckström, D.C., Eriksson Domellöf, M., Linder, J., Olsson, B., Öhrfelt, A., Trupp, M., Zetterberg, H., Blennow, K., and Forsgren, L. (2015). Cerebrospinal Fluid patterns and the risk of future dementia in early, incident Parkinson disease. JAMA Neurol. *72*, 1175–1182, http://dx.doi.org/10.1001/jamaneurol.2015.1449.

Barten, D.M., Cadelina, G.W., Hoque, N., DeCarr, L.B., Guss, V.L., Yang, L., Sankaranarayanan, S., Wes, P.D., Flynn, M.E., Meredith, J.E., et al. (2011). Tau transgenic mice as models for cerebrospinal fluid tau biomarkers. J. Alzheimers Dis. *24* (*Suppl 2*), 127–141, http://dx.doi.org/10.3233/JAD-2011-110161.

Boylan, K., Yang, C., Crook, J., Overstreet, K., Heckman, M., Wang, Y., Borchelt, D., and Shaw, G. (2009). Immunoreactivity of the phosphorylated axonal neurofilament H subunit (pNF-H) in blood of ALS model rodents and ALS patients: evaluation of blood pNF-H as a potential ALS biomarker. J. Neurochem. *111*, 1182–1191, http://dx.doi.org/10.1111/j.1471-4159.2009.06386.x.

Boylan, K.B., Glass, J.D., Crook, J.E., Yang, C., Thomas, C.S., Desaro, P., Johnston, A., Overstreet, K., Kelly, C., Polak, M., and Shaw, G. (2013). Phosphorylated neurofilament heavy subunit (pNF-H) in peripheral blood and CSF as a potential prognostic biomarker in amyotrophic lateral sclerosis. J. Neurol. Neurosurg. Psychiatry *84*, 467–472, http://dx.doi.org/10.1136/jnnp-2012-303768.

Del Tredici, K., and Braak, H. (2012). Lewy pathology and neurodegeneration in premotor Parkinson's disease. Mov. Disord. *27*, 597–607, http://dx.doi.org/10.1002/mds.24921.

Eggert, K.M., Oertel, W.H., and Reichmann, H. (2012). Leitlinien für Diagnoistik und Therapie in der Neurologie: Parkinson-Syndrome. Deutsche Gesellschaft für Neurologie, 1–48.

Eisele, Y.S., Obermüller, U., Heilbronner, G., Baumann, F., Kaeser, S.A., Wolburg, H., Walker, L.C., Staufenbiel, M., Heikenwalder, M., and Jucker, M. (2010). Peripherally applied Abeta-containing inoculates induce cerebral β-amyloidosis. Science *330*, 980–982, http://dx.doi.org/10.1126/science.1194516.

Gaiottino, J., Norgren, N., Dobson, R., Topping, J., Nissim, A., Malaspina, A., Bestwick, J.P., Monsch, A.U., Regeniter, A., Lindberg, R.L., et al. (2013). Increased neurofilament light chain blood levels in neurodegenerative neurological diseases. PLoS ONE *8*, e75091–e75099, http://dx.doi.org/10.1371/journal.pone.0075091.

Jack, C.R., Jr., and Holtzman, D.M. (2013). Biomarker modeling of Alzheimer's disease. Neuron *80*, 1347–1358, http://dx.doi.org/10.1016/j.neuron.2013.12.003.

Kuhle, J., Plattner, K., Bestwick, J.P., Lindberg, R.L., Ramagopalan, S.V., Norgren, N., Nissim, A., Malaspina, A., Leppert, D., Giovannoni, G., and Kappos, L. (2013). A comparative study of CSF neurofilament light and heavy chain protein in MS. Mult. Scler. *19*, 1597–1603, http://dx.doi.org/10.1177/1352458513482374.

Kuhle, J., Gaiottino, J., Leppert, D., Petzold, A., Bestwick, J.P., Malaspina, A., Lu, C.-H., Dobson, R., Disanto, G., Norgren, N., et al. (2015). Serum neurofilament light chain is a biomarker of human spinal cord injury severity and outcome. J. Neurol. Neurosurg. Psychiatry *86*, 273–279, http://dx.doi.org/10.1136/jnnp-2013-307454.

Lépinoux-Chambaud, C., and Eyer, J. (2013). Review on intermediate filaments of the nervous system and their pathological alterations. Histochem. Cell Biol. *140*, 13–22, http://dx.doi.org/10.1007/s00418-013-1101-1.

Leroy, K., Bretteville, A., Schindowski, K., Gilissen, E., Authelet, M., De Decker, R., Yilmaz, Z., Buée, L., and Brion, J.-P. (2007). Early axonopathy preceding neurofibrillary tangles in mutant tau transgenic mice. Am. J. Pathol. *171*, 976–992, http://dx.doi.org/10.2353/ajpath.2007.070345.

Lewis, J., McGowan, E., Rockwood, J., Melrose, H., Nacharaju, P., Van Slegtenhorst, M., Gwinn-Hardy, K., Paul Murphy, M., Baker, M., Yu, X., et al. (2000). Neurofibrillary tangles, amyotrophy and progressive motor disturbance in mice expressing mutant (P301L) tau protein. Nat. Genet. *25*, 402–405, http://dx.doi.org/10.1038/78078.

Liu, Q., Xie, F., Siedlak, S.L., Nunomura, A., Honda, K., Moreira, P.I., Zhua, X., Smith, M.A., and Perry, G. (2004). Neurofilament proteins in neurodegenerative diseases. Cell. Mol. Life Sci. *61*, 3057–3075, http://dx.doi.org/10.1007/s00018-004-4268-8.

Lu, C.-H., Petzold, A., Kalmar, B., Dick, J., Malaspina, A., and Greensmith, L. (2012). Plasma neurofilament heavy chain levels correlate to markers of late stage disease progression and treatment response in SOD1(G93A) mice that model ALS. PLoS ONE *7*, e40998–e13, http://dx.doi.org/10.1371/journal.pone.0040998.

Lu, C.-H., Macdonald-Wallis, C., Gray, E., Pearce, N., Petzold, A., Norgren, N., Giovannoni, G., Fratta, P., Sidle, K., Fish, M., et al. (2015). Neurofilament light chain: A prognostic biomarker in amyotrophic lateral sclerosis. Neurology *84*, 2247–2257, http://dx.doi.org/10.1212/WNL.0000000000001642.

Luk, K.C., Kehm, V.M., Zhang, B., O'Brien, P., Trojanowski, J.Q., and Lee, V.M.Y. (2012). Intracerebral inoculation of pathological α-synuclein initiates a rapidly progressive neurodegenerative α-synucleinopathy in mice. J. Exp. Med. *209*, 975–986, http://dx.doi.org/10.1084/jem.20112457.

Maetzler, W., Schmid, S.P., Wurster, I., Liepelt, I., Gaenslen, A., Gasser, T., and Berg, D. (2011). Reduced but not oxidized cerebrospinal fluid glutathione levels are lowered in Lewy body diseases. Mov. Disord. *26*, 176–181, http://dx.doi.org/10.1002/mds.23358.

Maia, L.F., Kaeser, S.A., Reichwald, J., Hruscha, M., Martus, P., Staufenbiel, M., and Jucker, M. (2013). Changes in amyloid-β and tau in the cerebrospinal fluid of transgenic mice overexpressing amyloid precursor protein. Sci. Transl. Med. *5*, 194re2, http://dx.doi.org/10.1126/scitranslmed.3006446.

Maia, L.F., Kaeser, S.A., Reichwald, J., Lambert, M., Obermüller, U., Schelle, J., Odenthal, J., Martus, P., Staufenbiel, M., and Jucker, M. (2015). Increased CSF Aβ during the very early phase of cerebral Aβ deposition in mouse models. EMBO Mol. Med. *7*, 895–903, http://dx.doi.org/10.15252/emmm.201505026.

Marek, K., Jennings, D., Tamagnan, G., and Seibyl, J. (2008). Biomarkers for Parkinson's [corrected] disease: tools to assess Parkinson's disease onset and progression. Ann. Neurol. *64* (*Suppl 2*), S111–S121, http://dx.doi.org/10.1002/ana.21602.

Martin, L.J., Pan, Y., Price, A.C., Sterling, W., Copeland, N.G., Jenkins, N.A., Price, D.L., and Lee, M.K. (2006). Parkinson's disease α-synuclein transgenic mice develop neuronal mitochondrial degeneration and cell death. J. Neurosci. *26*, 41–50, http://dx.doi.org/10.1523/JNEUROSCI.4308-05.2006.

Mattsson, N., Andreasson, U., Persson, S., Arai, H., Batish, S.D., Bernardini, S., Bocchio-Chiavetto, L., Blankenstein, M.A., Carrillo, M.C., Chalbot, S., et al. (2011). The Alzheimer's Association external quality control program for cerebrospinal fluid biomarkers. Alzheimers Dement. *7*, 386–395, http://dx.doi.org/10.1016/j.jalz.2011.05.2243.

McKhann, G.M., Knopman, D.S., Chertkow, H., Hyman, B.T., Jack, C.R., Jr., Kawas, C.H., Klunk, W.E., Koroshetz, W.J., Manly, J.J., Mayeux, R., et al. (2011). The diagnosis of dementia due to Alzheimer's disease: recommendations from the National Institute on Aging-Alzheimer's Association workgroups on diagnostic guidelines for Alzheimer's disease. Alzheimers Dement. *7*, 263–269, http://dx.doi.org/10.1016/j.jalz.2011.03.005.

Meyer-Luehmann, M., Coomaraswamy, J., Bolmont, T., Kaeser, S., Schaefer, C., Kilger, E., Neuenschwander, A., Abramowski, D., Frey, P., Jaton, A.L., et al. (2006). Exogenous induction of cerebral β-amyloidogenesis is governed by agent and host. Science *313*, 1781–1784, http://dx.doi.org/10.1126/science.1131864.

Mougenot, A.-L., Nicot, S., Bencsik, A., Morignat, E., Verchère, J., Lakhdar, L., Legastelois, S., and Baron, T. (2012). Prion-like acceleration of a synucleinopathy in a transgenic mouse model. Neurobiol. Aging *33*, 2225–2228, http://dx.doi.org/10.1016/j.neurobiolaging.2011.06.022.

Neselius, S., Brisby, H., Theodorsson, A., Blennow, K., Zetterberg, H., and Marcusson, J. (2012). CSF-biomarkers in Olympic boxing: diagnosis and effects of repetitive head trauma. PLoS ONE *7*, e33606–e33608, http://dx.doi.org/10.1371/journal.pone.0033606.

Neumann, M., Kahle, P.J., Giasson, B.I., Ozmen, L., Borroni, E., Spooren, W., Müller, V., Odoy, S., Fujiwara, H., Hasegawa, M., et al. (2002). Misfolded proteinase K-resistant hyperphosphorylated α-synuclein in aged transgenic mice with locomotor deterioration and in human α-synucleinopathies. J. Clin. Invest. *110*, 1429–1439, http://dx.doi.org/10.1172/JCI15777.

Neumann, U., Rueeger, H., Machauer, R., Veenstra, S.J., Lueoend, R.M., Tintelnot-Blomley, M., Laue, G., Beltz, K., Vogg, B., Schmid, P., et al. (2015). A novel BACE inhibitor NB-360 shows a superior pharmacological profile and robust reduction of amyloid-β and neuroinflammation in APP transgenic mice. Mol. Neurodegener. *10*, 44, http://dx.doi.org/10.1186/s13024-015-0033-8.

Petzold, A. (2005). Neurofilament phosphoforms: surrogate markers for axonal injury, degeneration and loss. J. Neurol. Sci. *233*, 183–198, http://dx.doi.org/10.1016/j.jns.2005.03.015.

Phinney, A.L., Horne, P., Yang, J., Janus, C., Bergeron, C., and Westaway, D. (2003). Mouse models of Alzheimer's disease: the long and filamentous road. Neurol. Res. *25*, 590–600, http://dx.doi.org/10.1179/016164103101202020.

Prodoehl, J., Li, H., Planetta, P.J., Goetz, C.G., Shannon, K.M., Tangonan, R., Comella, C.L., Simuni, T., Zhou, X.J., Leurgans, S., et al. (2013). Diffusion tensor imaging of Parkinson's disease, atypical parkinsonism, and essential tremor. Mov. Disord. *28*, 1816–1822, http://dx.doi.org/10.1002/mds.25491.

Radde, R., Bolmont, T., Kaeser, S.A., Coomaraswamy, J., Lindau, D., Stoltze, L., Calhoun, M.E., Jäggi, F., Wolburg, H., Gengler, S., et al. (2006). Abeta42-driven cerebral amyloidosis in transgenic mice reveals early and robust pathology. EMBO Rep. *7*, 940–946, http://dx.doi.org/10.1038/sj.embor.7400784.

Rojas, J.C., Karydas, A., Bang, J., Tsai, R.M., Blennow, K., Liman, V., Kramer, J.H., Rosen, H., Miller, B.L., Zetterberg, H., and Boxer, A.L. (2016). Plasma neurofilament light chain predicts progression in progressive supranuclear palsy. Ann. Clin. Transl. Neurol. *3*, 216–225, http://dx.doi.org/10.1002/acn3.290.

Sako, W., Murakami, N., Izumi, Y., and Kaji, R. (2015). Neurofilament light chain level in cerebrospinal fluid can differentiate Parkinson's disease from atypical parkinsonism: Evidence from a meta-analysis. J. Neurol. Sci. *352*, 84–87, http://dx.doi.org/10.1016/j.jns.2015.03.041.

Scherling, C.S., Hall, T., Berisha, F., Klepac, K., Karydas, A., Coppola, G., Kramer, J.H., Rabinovici, G., Ahlijanian, M., Miller, B.L., et al. (2014). Cerebrospinal fluid neurofilament concentration reflects disease severity in frontotemporal degeneration. Ann. Neurol. *75*, 116–126, http://dx.doi.org/10.1002/ana.24052.

Schweighauser, M., Bacioglu, M., Fritschi, S.K., Shimshek, D.R., Kahle, P.J., Eisele, Y.S., and Jucker, M. (2015). Formaldehyde-fixed brain tissue from spontaneously ill α-synuclein transgenic mice induces fatal α-synucleinopathy in transgenic hosts. Acta Neuropathol. *129*, 157–159, http://dx.doi.org/10.1007/s00401-014-1360-5.

Sperling, R., Mormino, E., and Johnson, K. (2014). The evolution of preclinical Alzheimer's disease: implications for prevention trials. Neuron *84*, 608–622, http://dx.doi.org/10.1016/j.neuron.2014.10.038.

Spittaels, K., Van den Haute, C., Van Dorpe, J., Bruynseels, K., Vandezande, K., Laenen, I., Geerts, H., Mercken, M., Sciot, R., Van Lommel, A., et al. (1999). Prominent axonopathy in the brain and spinal cord of transgenic mice overexpressing four-repeat human tau protein. Am. J. Pathol. *155*, 2153–2165, http://dx.doi.org/10.1016/S0002-9440(10)65533-2.

Steinacker, P., Feneberg, E., Weishaupt, J., Brettschneider, J., Tumani, H., Andersen, P.M., von Arnim, C.A., Böhm, S., Kassubek, J., Kubisch, C., et al. (2016). Neurofilaments in the diagnosis of motoneuron diseases: a prospective study on 455 patients. J. Neurol. Neurosurg. Psychiatry *87*, 12–20, http://dx.doi.org/10.1136/jnnp-2015-311387.

Vågberg, M., Norgren, N., Dring, A., Lindqvist, T., Birgander, R., Zetterberg, H., and Svenningsson, A. (2015). Levels and age dependency of neurofilament light and glial fibrillary acidic protein in healthy individuals and their relation to the brain parenchymal fraction. PLoS ONE *10*, e0135886–e0135888, http://dx.doi.org/10.1371/journal.pone.0135886.

Valentin, M.-A., Ma, S., Zhao, A., Legay, F., and Avrameas, A. (2011). Validation of immunoassay for protein biomarkers: bioanalytical study plan implementation to support pre-clinical and clinical studies. J. Pharm. Biomed. Anal. *55*, 869–877, http://dx.doi.org/10.1016/j.jpba.2011.03.033.

van der Putten, H., Wiederhold, K.H., Probst, A., Barbieri, S., Mistl, C., Danner, S., Kauffmann, S., Hofele, K., Spooren, W.P., Ruegg, M.A., et al. (2000). Neuropathology in mice expressing human alpha-synuclein. J. Neurosci. *20*, 6021–6029.

Vassar, R. (2014). BACE1 inhibitor drugs in clinical trials for Alzheimer's disease. Alzheimers Res. Ther. *6*, 89, http://dx.doi.org/10.1186/s13195-014-0089-7.

Winblad, B., Palmer, K., Kivipelto, M., Jelic, V., Fratiglioni, L., Wahlund, L.O., Nordberg, A., Bäckman, L., Albert, M., Almkvist, O., et al. 2004. Mild cognitive impairment—beyond controversies, towards a consensus: report of the International Working Group on Mild Cognitive Impairment., in. Presented at the Journal of internal medicine, pp. 240–246. http://dx.doi.org/10.1111/j.1365-2796.2004.01380.x.

Wirths, O., Weis, J., Szczygielski, J., Multhaup, G., and Bayer, T.A. (2006). Axonopathy in an APP/PS1 transgenic mouse model of Alzheimer's disease. Acta Neuropathol. *111*, 312–319, http://dx.doi.org/10.1007/s00401-006-0041-4.

Yuan, A., Rao, M.V., Veeranna, and Nixon, R.A. (2012a). Neurofilaments at a glance. J. Cell Sci. *125*, 3257–3263, http://dx.doi.org/10.1242/jcs.104729.

Yuan, A., Sasaki, T., Kumar, A., Peterhoff, C.M., Rao, M.V., Liem, R.K., Julien, J.-P., and Nixon, R.A. (2012b). Peripherin is a subunit of peripheral nerve neurofilaments: implications for differential vulnerability of CNS and peripheral nervous system axons. J. Neurosci. *32*, 8501–8508, http://dx.doi.org/10.1523/JNEUROSCI.1081-12.2012.

Yuan, A., Sershen, H., Veeranna, Basavarajappa, B.S., Kumar, A., Hashim, A., Berg, M., Lee, J.H., Sato, Y., Rao, M.V., et al. (2015). Neurofilament subunits are integral components of synapses and modulate neurotransmission and behavior in vivo. Mol. Psychiatry *20*, 986–994, http://dx.doi.org/10.1038/mp.2015.45.

Zetterberg, H., Skillbäck, T., Mattsson, N., Trojanowski, J.Q., Portelius, E., Shaw, L.M., Weiner, M.W., and Blennow, K.; Alzheimer's Disease Neuroimaging Initiative (2016). Association of cerebrospinal fluid neurofilament light concentration with Alzheimer disease progression. JAMA Neurol. *73*, 60–67, http://dx.doi.org/10.1001/jamaneurol.2015.3037.